

# A comprehensive prediction model of drug-refractory epilepsy based on combined clinical-EEG microstate features

Jinying Zhang\*, Chaofeng Zhu\*, Juan Li\*, Luyan Wu, Yuying Zhang, Huapin Huang and Wanhui Lin 

*Ther Adv Neurol Disord*

2024, Vol. 17: 1–21

DOI: 10.1177/  
17562864241276202

© The Author(s), 2024.  
Article reuse guidelines:  
sagepub.com/journals-  
permissions

## Abstract

**Background:** Epilepsy is a chronic neurological disorder characterized by recurrent seizures that significantly impact patients' quality of life. Identifying predictors is crucial for early intervention.

**Objective:** Electroencephalography (EEG) microstates effectively describe the resting state activity of the human brain using multichannel EEG. This study aims to develop a comprehensive prediction model that integrates clinical features with EEG microstates to predict drug-refractory epilepsy (DRE).

**Design:** Retrospective study.

**Methods:** This study encompassed 226 patients with epilepsy treated at the epilepsy center of a tertiary hospital between October 2020 and May 2023. Patients were categorized into DRE and non-DRE groups. All patients were randomly divided into training and testing sets. Lasso regression combined with Stepglm [both] algorithms was used to screen independent risk factors for DRE. These risk factors were used to construct models to predict the DRE. Three models were constructed: a clinical feature model, an EEG microstate model, and a comprehensive prediction model (combining clinical-EEG microstates). A series of evaluation methods was used to validate the accuracy and reliability of the prediction models. Finally, these models were visualized for display.

**Results:** In the training and testing sets, the comprehensive prediction model achieved the highest area under the curve values, registering 0.99 and 0.969, respectively. It was significantly superior to other models in terms of the C-index, with scores of 0.990 and 0.969, respectively. Additionally, the model recorded the lowest Brier scores of 0.034 and 0.071, respectively, and the calibration curve demonstrated good consistency between the predicted probabilities and observed outcomes. Decision curve analysis revealed that the model provided significant clinical net benefit across the threshold range, underscoring its strong clinical applicability. We visualized the comprehensive prediction model by developing a nomogram and established a user-friendly website to enable easy application of this model ([https://fydxh.shinyapps.io/CE\\_model\\_of\\_DRE/](https://fydxh.shinyapps.io/CE_model_of_DRE/)).

**Conclusion:** A comprehensive prediction model for DRE was developed, showing excellent discrimination and calibration in both the training and testing sets. This model provided an intuitive approach for assessing the risk of developing DRE in patients with epilepsy.

**Keywords:** drug-refractory epilepsy, electroencephalography microstates, Lasso, nomogram, prediction model, Stepglm

Correspondence to:

**Wanhui Lin**  
Department of Neurology,  
Fujian Medical University  
Union Hospital, Xinquan  
Road 29#, Fuzhou, Fujian  
Province, China

Fujian Key Laboratory  
of Molecular Neurology,  
Fuzhou, China  
[wanhuilin@fjmu.edu.cn](mailto:wanhuilin@fjmu.edu.cn)

**Huapin Huang**  
Department of Neurology,  
Fujian Medical University  
Union Hospital, Xinquan  
Road 29#, Fuzhou, Fujian  
Province, China

Fujian Key Laboratory  
of Molecular Neurology,  
Fuzhou, China

Department of Geriatrics,  
Fujian Medical University  
Union Hospital, Fuzhou,  
China  
[hh-p@163.com](mailto:hh-p@163.com)

**Jinying Zhang**  
Department of Neurology,  
Fujian Medical University  
Union Hospital, Fuzhou,  
China

Department of Neurology,  
The Second Affiliated  
Hospital of Fujian Medical  
University, Quanzhou,  
Fujian Province, China

**Chaofeng Zhu**  
**Juan Li**  
**Luyan Wu**  
**Yuying Zhang**  
Department of Neurology,  
Fujian Medical University  
Union Hospital, Fuzhou,  
China

\* Co-first-authors: Jinying  
Zhang, Chaofeng Zhu, and  
Juan Li contributed equally

Received: 14 May 2024; revised manuscript accepted: 31 July 2024.



## Introduction

Epilepsy is a chronic neurological disorder characterized by recurrent episodes of abnormal and excessive electrical discharge in the brain, leading to transient central nervous system dysfunction.<sup>1</sup> Unfortunately, around 30% of these patients do not respond to conventional antiseizure medication (ASM) and develop drug-refractory epilepsy (DRE).<sup>1</sup> Prolonged or frequent seizures, as well as status epilepticus, can severely impact patients' cognition, memory, quality of life, and psychological well-being.<sup>1</sup> The International League Against Epilepsy (ILAE) defines DRE as the failure of two well-tolerated and appropriately selected antiseizure medication regimens, used alone or in combination, to achieve sustained seizure freedom.<sup>2</sup> Consequently, early diagnosis of DRE is crucial to improve patient outcomes.<sup>3</sup>

The development of DRE is associated with various factors, including specific types of epilepsy syndromes, age of onset, multiple seizure types, clear neuroimaging abnormalities such as hippocampal sclerosis, cortical dysplasia, tumors, and traumatic lesions, widespread epileptiform electroencephalography (EEG) changes, and previous treatment failure with ASMs.<sup>4,5</sup> Several prediction models and predictors have been proposed to improve clinical outcomes for patients with DRE. However, the currently available indicators for guiding clinical practice are still limited due to their lack of specificity and sensitivity, limited generalizability, and high cost.

EEG is the most important tool for diagnosing and distinguishing epilepsy. Research has shown that spontaneous brain activity during resting state accounts for 80% of total brain energy.<sup>6</sup> Resting-state EEG analysis involves various methods such as power spectrum analysis,<sup>7</sup> whole-brain domain synchronization,<sup>8</sup> functional network connectivity,<sup>9</sup> and EEG microstates.<sup>10</sup> EEG microstates are an effective method for describing the resting state activity of the human brain using multichannel EEG.<sup>10</sup> The concept of EEG microstates originated from the observation that broad-band spontaneous EEG activity during rest can be characterized by a finite set of scalp potential topographies.<sup>10</sup> These configurations remain quasi-stable for a distinct duration before swiftly transitioning into a new topographical arrangement.<sup>11</sup> These periods of quasi-stability, reflecting the pace at which humans process information, are known as microstates.<sup>12</sup> These

microstates signal the “near-simultaneous activity among nodes within large-scale networks.”<sup>12</sup> Each microstate typically lasting 60–120 ms.<sup>13</sup> About 70% of EEG signals can be adequately represented by four microstates, labeled as A, B, C, and D.<sup>8,14</sup> Microstate A connects to brain activity in the temporal cortex and left insula, suggesting a function in language processing.<sup>15,16</sup> Microstate B, linked to the occipital region, is involved in visual processing.<sup>15,16</sup> EEG activity in the cingulate gyrus, inferior frontal gyrus, insula, and precuneus gyrus associates with microstate C, which participates in subjective perception and autonomic processing.<sup>15</sup> Microstate D is thought to be involved in attention and analytical processing and has been shown to be linked to neural activity in the right hemispheric regions of the frontal and parietal cortices.<sup>15</sup>

EEG microstate measures, including average duration, coverage, frequency, and transition probability (TP), describe changes in brain states and reflect abnormalities in brain network function.<sup>10,17</sup> EEG microstate analysis has been extensively applied in the field of neuropsychiatric disorders, including schizophrenia,<sup>18</sup> dementia,<sup>19</sup> and narcolepsy.<sup>20</sup> These findings suggest that EEG microstate analysis could serve as an effective tool for identifying abnormalities associated with brain disorders.<sup>19,20</sup> Although EEG microstate is commonly employed to examine brain function, its application in studying DRE through EEG microstate analysis has been relatively underexplored. Functional connections between subcortical and cortical structures undergo alterations during epileptic seizures. These changes imply shifts in patterns of brain activity, which may offer valuable insights into microstate variations after seizures.<sup>21</sup>

While various predictive models for DRE exist,<sup>22</sup> none currently combines clinical features with EEG microstates. This study aimed to develop a nomogram model by integrating clinical features with EEG microstates, and to assess the model's performance in predicting DRE. This approach aims to offer novel reference indicators for the diagnosis of DRE.

## Materials and methods

### *Participants and data acquisition*

*Participants.* We retrospectively investigated a total of 226 patients with epilepsy who were

treated between October 2020 and May 2023 at the epilepsy center of Fujian Medical University Union Hospital. The inclusion criteria were as follows: (1) Patients who met the ILAE's definition of epilepsy<sup>2</sup>; (2) patients who underwent video electroencephalography (VEEG) monitoring; (3) patients with a complete medical history, neurological examination, and magnetic resonance imaging (MRI) data; and (4) patients who regularly took ASMs. The ASMs administered to patients in this study included sodium valproate, oxcarbazepine, carbamazepine, levetiracetam, lamotrigine, perampanel, topiramate, phenytoin, phenobarbital, and clonazepam. The exclusion criteria were as follows: (1) patients lacking VEEG monitoring; (2) patients with incomplete medical records; (3) patients suffering from severe liver or kidney disease; and (4) patient with irregular ASMs therapy and poor compliance.

The patients were categorized into two groups based on their follow-up records, as shown in Figure 1. Participants were enrolled in the non-DRE (NDRE) group ( $n=77$ ) if they achieved freedom from all types of seizures for 12 months or three times the pre-intervention interseizure interval, whichever was longer, after receiving appropriate ASM therapy.<sup>2</sup> Participants were enrolled in the DRE group ( $n=149$ ) after failing to achieve sustained seizure freedom despite adequate trials of two ASM regimens, which were both tolerated and appropriately chosen and used, whether as monotherapies or in combination.<sup>2</sup>

### Clinical features

This study includes the following clinical feature variables: continuous variables and categorical variables. Continuous variables included: age, body mass index (BMI), educational years, age at onset, and duration of epilepsy. Categorical variables included: (1) gender; (2) educational level (primary, senior, college, or above); (3) family history of epilepsy; (4) type of epilepsy (focal, generalized, focal secondary generalized, multiple, and unknown onset); and (5) initial seizure frequency. Initial seizure frequency is referred to as the frequency of patients' experience before starting treatment with ASMs, categorized as follows: (1) Daily: the patient experienced seizures every day. (2) Weekly: the patient experienced at least one seizure every week. (3) Monthly: the patient experienced at least one seizure every

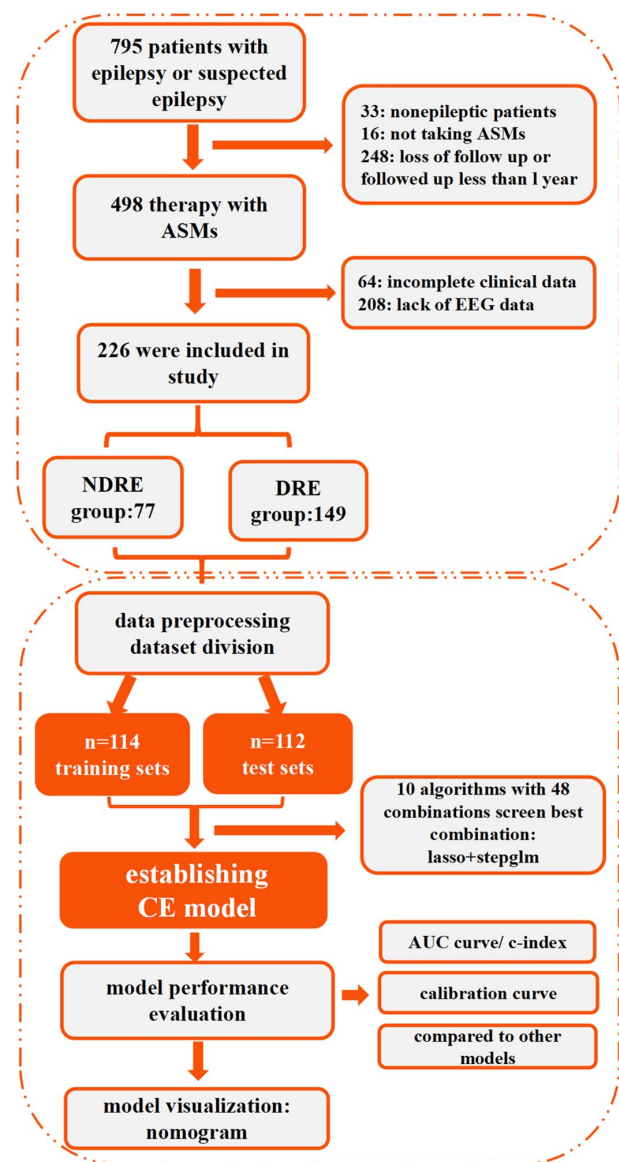


**Figure 1.** Flow chart.

ASM, antiseizure medication; AUC, area under the curve; CE, clinical and EEG microstate features; DRE group, drug-refractory epilepsy group; EEG, electroencephalography; NDRE group, non-drug-refractory epilepsy group.

month. (4) Yearly : the patient experienced seizures at intervals longer than a month, not fitting into the daily, weekly, or monthly categories. (5) Etiology (genetic, structural, immunological, metabolic, infectious, and unknown). (6) History of status epilepticus. (7) History of generalized tonic-clonic seizures (GTCS). (8) Nocturnal seizures. (9) History of febrile seizures. (10) EEG findings: results of an EEG examination, categorized as normal EEG (1), EEG with abnormal background (2), and EEG with epileptiform

discharge (3). (11) MRI findings: MRI positivity indicates radiological abnormalities related to epilepsy, the epilepsy-related radiological abnormalities primarily included the following: brain tumors, stroke lesions, vascular malformations, hippocampal sclerosis, cortical dysplasia, post-traumatic lesions, central nervous system infection. (12) Absence epilepsy. (13) Comorbid cognitive disorder. The Montreal Cognitive Assessment (MoCA) and Mini-Mental State Examination (MMSE) were used to assess cognition. MMSE  $\leq 19$  for illiterates,  $\leq 22$  for those with elementary school education, and  $\leq 26$  for those with junior high school education and above. According to the Chinese MoCA criteria, illiterates  $\leq 13$ , those with 1–6 years of education  $\leq 19$ , and those with 7 or more years of education  $\leq 24$ .<sup>23</sup> (14) Comorbid Psychiatric disorder. (15) Comorbid depression. The Self-rating Depression Scale (SDS) was employed to evaluate depression. SDS index scores of 25–49 (raw score 20–40) were normal; SDS index scores of 50 or more (raw score = 40) indicated the presence of depressive symptoms.<sup>24</sup>

#### *EEG acquisition and preprocessing*

*Resting-state EEG acquisition.* Subjects washed their hair prior to EEG collection, refrained from using oily cleaning or hair care products, recorded their scalp EEG in a quiet and relaxed state. All patients with epilepsy underwent VEEG recording. To avoid slow waves caused by hunger, patients were required to have normal meals during the monitoring period. EEG data were recorded continuously for 24 h, and a 10-min segment of EEG data during which the patients were awake was extracted for analysis.

VEEG recordings were performed using an EEG recorder (EEG-1200C, Japan) with 19 scalp electrodes and two reference electrodes placed strictly according to the international 10/20 system. Video and EEG data were recorded in a synchronized manner. Electrodes (Fp1, Fp2, F3, F4, F7, F8, T7, T8, P7, P8, C3, C4, P3, P4, O1, O2, Fz, Cz, and Pz) were positioned precisely using a standardized ruler.<sup>21</sup> The electrical impedance of the scalp electrodes was less than 5 k $\Omega$ . The EEG-1200C had a sampling rate of 500 Hz, the low-pass filter rate was 70 Hz, and the high-pass filter rate was 0.5 Hz. Epileptic seizures and epileptiform discharges were analyzed and marked by two experienced EEG technicians.

#### *EEG data preprocessing*

The preprocessing of EEG data was carried out using Matlab R2013b software (MathWorks, Inc., Natick, MA, USA) equipped with the EEGLAB toolbox.<sup>25</sup> The steps involved in preprocessing are as follows: (1) Importing raw data: the raw EEG data were first imported into the EEGLAB toolbox. (2) Electrode localization: we localized the electrodes according to the standard 10–20 system. (3) Interpolating bad electrodes: any electrodes with poor signal quality were interpolated to ensure data consistency. (4) Removing time segments with excessive drift: time segments with excessive drift or noise were identified and removed to enhance data quality. (5) Downsampling: the continuous EEG data were downsampled to 250 Hz to reduce computational load while retaining essential signal information. (6) Segmentation into epochs: the downsampled EEG data were segmented into 2-s epochs to facilitate analysis. (7) Band-pass filtering: a band-pass filter was set from 1 to 40 Hz to focus on the frequency range of interest, which includes most of the relevant brain wave frequencies. (8) Notch filtering: a notch filter was applied at 50 Hz to eliminate line noise commonly found in EEG recordings. (9) Artifact removal using independent component analysis (ICA): ICA was employed to effectively remove artifacts caused by eye movements, heartbeats, and muscle activity, thereby improving the signal quality for subsequent analysis. (10) Readjusting the filter: finally, the filter was readjusted to 2–20 Hz to further refine the signal for the microstate analysis. For each patient, we retained 3 min of EEG data, which correspond to a total of 90 epochs.<sup>26</sup>

#### *EEG microstate analysis*

EEG microstate analysis was performed using Cartool software following EEG data preprocessing,<sup>27</sup> adhering to a standardized procedure from previous studies.<sup>28,29</sup> The analysis involved three principal steps: First, we computed the global field power (GFP) to assess potential variations across electrodes at specific time points.<sup>14</sup> When GFP reaches its peak, the EEG topography is deemed stable, and these topographies are defined as microstates.<sup>14</sup> Subsequently, clustering analysis was applied to the GFP's local maxima.<sup>14,28</sup> The topographical maps at these GFP peaks were recognized as unique microstates, illustrating the dynamic shifts in EEG signals as transitions occur between these states.<sup>27</sup> Utilizing a modified

version of the K-means clustering algorithm,<sup>30</sup> we identified four distinct microstate topographies: A, B, C, and D. Finally, we calculated four parameters for each microstate—duration, frequency, coverage, and TPs<sup>14</sup>—to collectively depict variations in the brain’s states.

Duration referred to the average length of time (in milliseconds) during which a given EEG microstate remains stable/present, reflecting the stability of neural activity in the cerebral cortex.<sup>14</sup> Frequency represented the number of times an EEG microstate repeats within 1 s (in occurrences per second), indicative of the frequency or tendency of activation in the underlying neural populations or systems.<sup>14</sup> Coverage represented the percentage of total time covered by a specific EEG microstate category (in percentages).<sup>14</sup> TPs indicated the probabilities of transitions between different EEG microstates (in percentages).<sup>14</sup>

### *Modeling process*

After completing the above steps, we used the “createDataPartition” function from the “caret” package to split the dataset into training and testing sets in a 0.5:0.5 ratio. We randomly selected 50% of the NDRE group (39 cases) and 50% of the DRE group (75 cases) to form the training set, totaling 114 samples. The remaining 50% of the dataset, consisting of 38 NDRE patients and 74 DRE patients, comprised the test set, totaling 112 samples.

To establish and validate a comprehensive model for predicting DRE, we employed multiple machine learning algorithms. Initially, we integrated 10 algorithms: Lasso, Ridge, Elastic Net (Enet), Stepwise GLM (Stepglm), support vector machine (SVM), glmBoost, linear discriminant analysis (LDA), random forest (RF), gradient boosting machine (GBM), and naïve Bayes.<sup>31</sup> We then created 48 combinations of these algorithms. In each combination, the first algorithm was used for important variable selection, and the second algorithm was further used for refinement and modeling. The important variables identified varied across different algorithm combinations (Supplemental Table).

To reduce random errors in data partitioning, prevent information leakage, and

ensure algorithm stability, we used a 10-fold cross-validation method.<sup>32</sup> Utilizing the “createMultiFolds” function from the “caret” package, we performed 10-fold cross validation repeated 200 times. The dataset was randomly divided into 10 subsets (“folds”), with 9 subsets used for training and 1 subset used for testing. This process was repeated 10 times, with each subset used as the test set once.<sup>32</sup> By averaging the performance metrics across all folds, we ensured that the model’s evaluation is robust and not dependent on a specific data split, ultimately aiding in the selection of the most optimal model.

The initial training of the models was conducted on the training set, followed by testing the model performance on the test set. Each model’s performance was assessed by calculating Harrell’s concordance index (C-index), and the model with the highest average C-index was selected as the optimal model. In this study, three predictive models for DRE were constructed: (1) a clinical model, consisting solely of clinical features; (2) an EEG model, based solely on EEG microstate feature parameters; and (3) a CE model, combining clinical features with EEG microstate analysis feature parameters.

To compare the performance of the three predictive models with other models, we retrieved published models by searching PubMed for articles published. We used the following Boolean terms for our search: (“epilepsy” OR “seizure” OR “convulsion”) AND (“refractory” OR “drug-resistant” OR “pharmacoresistant” OR “intractable” OR “drug response” OR “prognosis”) AND (“risk factor” OR “predictor” OR “predictive”). We then selected original publications that established models relevant as comparisons to the three DRE predictive models.<sup>33–60</sup>

### *Model performance evaluation*

For each model, the concordance index (C-index) or area under the curve (AUC) was calculated across all datasets, and the model boasting the highest average C-index or AUC was deemed the optimal model. These results were then benchmarked against multiple existing prediction models. To assess the agreement between the model’s predicted outcomes and actual results, a calibration curve was plotted. Decision curve analysis (DCA) was performed to evaluate the utility of these models.

Additionally, a nomogram and a website were developed to visualize the model's structure.

### Statistical analysis

All data processing, statistical analysis, and graphing were conducted using R software version 4.2.2. (R Foundation for Statistical Computing, <https://www.r-project.org>) Continuous variables were presented as mean  $\pm$  standard deviation and categorical variables were presented as  $n$  (%). Continuous variables were tested using Student's  $t$ -test or one-way ANOVA, as appropriate. Categorical variables were tested using the Chi-square test or Fisher's exact test, as appropriate. Feature correlations were calculated using the Pearson correlation coefficient, with visualization performed using heatmaps. The "createDataPartition" function from the "caret" package was used to split the dataset into training and testing sets in a 0.5:0.5 ratio. The Receiver Operating Characteristic (ROC) curve for predicting binary classification variables was implemented using the "pROC" package in R software. Figures were drawn using the "ggplot2" and "Regplot" packages. The "shiny" package is employed to create a web calculator, providing users with an interactive data analysis tool. The false discovery rate (FDR) was employed for multiple test correction. A  $p$ -value of  $<0.05$  was considered statistically significant.

## Results

### Patients characteristics

A total of 226 patients were included in the study, including 110 males and 116 females, with an average age of  $32.465 \pm 14.166$  years. The NDRE group consisted of 77 patients, including 39 males (50.65%) and 38 females (49.35%), with an average age of  $32.234 \pm 16.351$  years. The DRE group consisted of 149 patients, including 71 males (47.65%) and 78 females (52.35%), with an average age of  $32.584 \pm 12.952$  years.

### Description of clinical features and analysis of EEG microstate features

The results showed no significant differences between the NDRE and DRE groups in terms of gender, age, BMI, educational level and years, family history of epilepsy, type of epilepsy, etiology of epilepsy, history of status epilepticus,

history of GTCS, nocturnal seizures, history of febrile seizures, MRI findings, comorbid cognitive disorders, and comorbid psychiatric disorders (all  $p > 0.05$ ). However, significant differences were observed in the duration of epilepsy, age at onset, initial seizure frequency, abnormal EEG findings, absence epilepsy, and comorbid depression between the two groups (all  $p < 0.01$ ), as demonstrated in Table 1 and Figure 2. After applying the FDR for multiple testing correction, statistically significant differences in the duration of epilepsy, initial seizure frequency, EEG findings, absence epilepsy, and comorbid depression between the two groups were still evident.

The microstate maps were classified into four distinct categories as A, B, C, and D. Supplemental Figure visually presents the microstate topographic classes observed within the DRE group and NDRE group.

For microstates B and D, the differences in duration, frequency, and coverage between the two groups were statistically significant. The average duration, frequency, and coverage of microstate B in the DRE group were higher than those in the NDRE group. Conversely, the three indicators for microstate D were lower in the DRE group compared to the NDRE group. The duration of microstate C was statistically significantly shorter in the DRE group than in the NDRE group. For microstate A, the differences in duration, frequency, and coverage between the two groups were not statistically significant (all  $p > 0.05$ ). The TPs between the two groups were statistically significant (all  $p < 0.001$ ), as demonstrated in Table 2 and Figure 3. After applying the FDR for multiple testing correction, these differences were still found to be statistically significant.

To investigate the correlations among feature variables, we calculated the correlation coefficients between two groups of distinct variables and visualized the results. The results are presented in Supplemental Figures 1 and 2.

### Model establishment

We integrated 10 machine learning algorithms and 48 algorithm combinations. The AUC was computed for each algorithm. Select the algorithm with the highest average AUC as the optimal algorithm. The evaluation results of the algorithms were then visually presented using a

**Table 1.** Baseline epilepsy patient characteristics in the DRE and NDRE groups.

| Characteristic                 | Level                         | Overall         | NDRE            | DRE             | <i>p</i> -Adjust |
|--------------------------------|-------------------------------|-----------------|-----------------|-----------------|------------------|
| <i>n</i>                       |                               | 226             | 77              | 149             |                  |
| Gender (%)                     | Female                        | 116 (51.33)     | 38 (49.35)      | 78 (52.35)      | 0.7741           |
|                                | Male                          | 110 (48.67)     | 39 (50.65)      | 71 (47.65)      |                  |
| Age (years)                    |                               | 32.465 (14.166) | 32.234 (16.351) | 32.584 (12.952) | 0.9021           |
| BMI (kg/m <sup>2</sup> )       |                               | 21.870 (3.435)  | 21.562 (3.045)  | 22.029 (3.619)  | 0.3435           |
| Educational level (%)          | Primary                       | 40 (17.70)      | 12 (15.58)      | 28 (18.79)      | 0.7478           |
|                                | Senior                        | 113 (50.00)     | 38 (49.35)      | 75 (50.34)      |                  |
|                                | College or above              | 73 (32.30)      | 27 (35.06)      | 46 (30.87)      |                  |
| Educational years              |                               | 10.606 (3.629)  | 11.143 (3.772)  | 10.329 (3.534)  | 0.1488           |
| Family history of epilepsy (%) | No                            | 16 (7.08)       | 3 (3.90)        | 13 (8.72)       | 0.2856           |
|                                | Yes                           | 210 (92.92)     | 74 (96.10)      | 136 (91.28)     |                  |
| Duration of epilepsy (years)   |                               | 11.641 (9.792)  | 7.414 (7.433)   | 13.825 (10.164) | <0.0001          |
| Age at onset (years)           |                               | 20.537 (14.912) | 24.279 (16.630) | 18.603 (13.600) | 0.0158           |
| Type of epilepsy (%)           | Focal                         | 67 (29.65)      | 19 (24.68)      | 48 (32.21)      | 0.6836           |
|                                | Generalized                   | 18 (7.96)       | 6 (7.79)        | 12 (8.05)       |                  |
|                                | F_to_G                        | 29 (12.83)      | 11 (14.29)      | 18 (12.08)      |                  |
|                                | Multiple                      | 47 (20.80)      | 15 (19.48)      | 32 (21.48)      |                  |
|                                | unknown                       | 65 (28.76)      | 26 (33.77)      | 39 (26.17)      |                  |
|                                | Initial seizure frequency (%) | Daily           | 23 (10.18)      | 0 (0.00)        |                  |
|                                | Weekly                        | 14 (6.19)       | 0 (0.00)        | 14 (9.40)       |                  |
|                                | Monthly                       | 55 (24.34)      | 4 (5.19)        | 51 (34.23)      |                  |
|                                | Yearly                        | 134 (59.29)     | 73 (94.81)      | 61 (40.94)      |                  |
| Etiology (%)                   | Genetic                       | 6 (2.65)        | 1 (1.30)        | 5 (3.36)        | 0.2735           |
|                                | Structural                    | 65 (28.76)      | 21 (27.27)      | 44 (29.53)      |                  |
|                                | Infectious                    | 4 (1.77)        | 3 (3.90)        | 1 (0.67)        |                  |
|                                | unknown                       | 151 (66.81)     | 52 (67.53)      | 99 (66.44)      |                  |
| History of SE (%)              | No                            | 186 (82.30)     | 63 (81.82)      | 123 (82.55)     | 1                |
|                                | Yes                           | 40 (17.70)      | 14 (18.18)      | 26 (17.45)      |                  |
| History of GTCS (%)            | No                            | 59 (26.11)      | 20 (25.97)      | 39 (26.17)      | 1                |
|                                | Yes                           | 167 (73.89)     | 57 (74.03)      | 110 (73.83)     |                  |

*(Continued)*

**Table 1.** (Continued)

| Characteristic                     | Level                   | Overall     | NDRE       | DRE         | p-Adjust |
|------------------------------------|-------------------------|-------------|------------|-------------|----------|
| Nocturnal seizure (%)              | No                      | 80 (35.40)  | 25 (32.47) | 55 (36.91)  | 0.6062   |
|                                    | Yes                     | 146 (64.60) | 52 (67.53) | 94 (63.09)  |          |
| History of febrile seizure (%)     | No                      | 189 (83.63) | 66 (85.71) | 123 (82.55) | 0.6748   |
|                                    | Yes                     | 37 (16.37)  | 11 (14.29) | 26 (17.45)  |          |
| EEG findings (%)                   | Normal                  | 27 (11.95)  | 18 (23.38) | 9 (6.04)    | 0.0007   |
|                                    | Abnormal background     | 4 (1.77)    | 1 (1.30)   | 3 (2.01)    |          |
|                                    | Epileptiform discharges | 195 (86.28) | 58 (75.32) | 137 (91.95) |          |
| MRI findings (%)                   | Negative                | 157 (69.47) | 57 (74.03) | 100 (67.11) | 0.3592   |
|                                    | Positive                | 69 (30.53)  | 20 (25.97) | 49 (32.89)  |          |
| Absence epilepsy (%)               | No                      | 191 (84.51) | 73 (94.81) | 118 (79.19) | 0.004    |
|                                    | Yes                     | 35 (15.49)  | 4 (5.19)   | 31 (20.81)  |          |
| Comorbid cognitive disorder (%)    | No                      | 38 (16.81)  | 8 (10.39)  | 30 (20.13)  | 0.0952   |
|                                    | Yes                     | 188 (83.19) | 69 (89.61) | 119 (79.87) |          |
| Comorbid psychiatric disorders (%) | No                      | 8 (3.54)    | 1 (1.30)   | 7 (4.70)    | 0.3519   |
|                                    | Yes                     | 218 (96.46) | 76 (98.70) | 142 (95.30) |          |
| Comorbid depression (%)            | No                      | 72 (31.86)  | 15 (19.48) | 57 (38.26)  | 0.0065   |
|                                    | Yes                     | 154 (68.14) | 62 (80.52) | 92 (61.74)  |          |

DRE, drug-refractory epilepsy; EEG, electroencephalography; GTCS, generalized tonic-clonic seizures; MRI: magnetic resonance imaging; n, number of patients; NDRE, non-drug-refractory epilepsy group; SE, status epilepticus.

heatmap (Figure 4(a)). Interestingly, the optimal algorithm was a combination of Lasso and Stepglm (direction = both) with the highest average AUC (0.98) (Figure 4(a)).

Next, we used the combination of the Lasso and Stepglm [both] algorithms to train the training set and the test set. The first step involved variable selection from numerous potential influencing factors, performed using Lasso regression. Lasso regression analysis relies on the selection of the regularization parameter lambda, which applies penalty terms to reduce the coefficients of certain variables to zero. This process achieves sparse selection of variables and effectively

screens out predictive factors related to the outcome variable.<sup>31</sup> The optimal lambda value, minimizing the model's average prediction error, was identified through cross validation (Figure 4(b)). With variables selected by Lasso regression, the model was further refined using Stepglm [both], which determined the key variables for the predictive model through a stepwise method of adding and deleting variables<sup>31</sup>(Figure 4(c)).

#### Clinical model

A total of eight features were included in the model: the duration of epilepsy, initial seizure



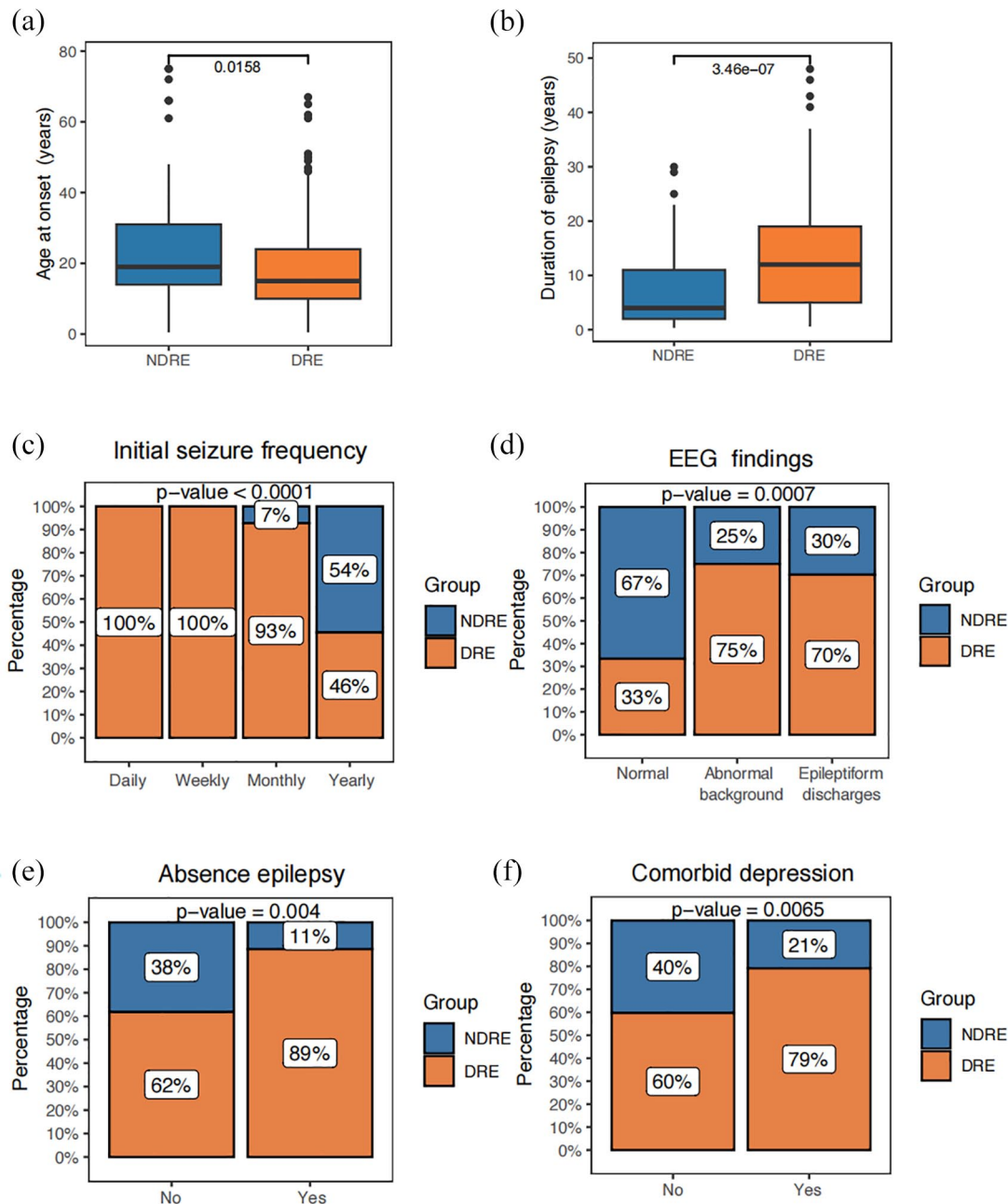


**Figure 2.** Clinical features. Compare the age at onset, duration of epilepsy, initial seizure frequency, EEG findings, absence epilepsy, and comorbid depression between the two groups: (a) correspond to the age at onset, (b) correspond to the duration of epilepsy, (c) correspond to the initial seizure frequency, (d) correspond to the EEG findings, (e) correspond to the absence epilepsy, and (f) correspond to comorbid depression. DRE, drug-refractory epilepsy; EEG, electroencephalography; NDRE, non-drug-refractory epilepsy.

frequency, EEG findings, absence epilepsy, comorbid psychiatric disorders, and comorbid depression. The C-index [95% confidence interval] for the training set was 0.865 [0.801–0.929], and for the test set, it was 0.861 [0.788–0.94].

#### EEG model

A total of 10 features were included in the model. These features consist of the durations of microstates A, C, and D, along with the TPs from microstate A to C, A to D, B to D, C to D, D to A, D to B, and D to C. The C-index, which

**Table 2.** Comparison of EEG microstate features between NDRE and DRE groups.

| Variables         | Level     | Overall          | NDRE             | DRE              | p-Adjust |
|-------------------|-----------|------------------|------------------|------------------|----------|
| Microstate A      | Duration  | 114.536 (12.916) | 114.440 (12.456) | 114.586 (13.189) | 0.9358   |
|                   | Coverage  | 28.391 (6.960)   | 28.807 (6.855)   | 28.176 (7.027)   | 0.5553   |
|                   | Frequency | 3.982 (0.617)    | 4.054 (0.661)    | 3.944 (0.592)    | 0.2564   |
| Microstate B      | Duration  | 104.034 (10.649) | 96.671 (9.800)   | 107.839 (8.962)  | <0.0001  |
|                   | Coverage  | 23.557 (5.831)   | 18.170 (4.792)   | 26.341 (4.122)   | <0.0001  |
|                   | Frequency | 3.702 (0.696)    | 3.109 (0.586)    | 4.008 (0.532)    | <0.0001  |
| Microstate C      | Duration  | 101.333 (11.400) | 103.460 (10.185) | 100.234 (11.864) | 0.0476   |
|                   | Coverage  | 21.442 (5.390)   | 22.335 (5.166)   | 20.981 (5.462)   | 0.0910   |
|                   | Frequency | 3.481 (0.540)    | 3.553 (0.487)    | 3.443 (0.563)    | 0.1547   |
| Microstate D      | Duration  | 110.103 (15.440) | 117.878 (17.627) | 106.086 (12.457) | <0.0001  |
|                   | Coverage  | 26.610 (5.909)   | 30.689 (5.497)   | 24.502 (4.943)   | <0.0001  |
|                   | Frequency | 3.925 (0.535)    | 4.216 (0.485)    | 3.775 (0.497)    | <0.0001  |
| TP of microstates | A→B       | 0.090 (0.027)    | 0.071 (0.015)    | 0.099 (0.026)    | <0.0001  |
|                   | A→C       | 0.080 (0.015)    | 0.084 (0.016)    | 0.077 (0.014)    | 0.0013   |
|                   | A→D       | 0.094 (0.026)    | 0.115 (0.027)    | 0.084 (0.017)    | <0.0001  |
|                   | B→A       | 0.089 (0.026)    | 0.070 (0.014)    | 0.098 (0.026)    | <0.0001  |
|                   | B→C       | 0.071 (0.016)    | 0.062 (0.013)    | 0.075 (0.016)    | <0.0001  |
|                   | B→D       | 0.085 (0.018)    | 0.076 (0.018)    | 0.090 (0.016)    | <0.0001  |
|                   | C→A       | 0.080 (0.015)    | 0.086 (0.017)    | 0.077 (0.013)    | <0.0001  |
|                   | C→B       | 0.070 (0.017)    | 0.060 (0.014)    | 0.075 (0.016)    | <0.0001  |
|                   | C→D       | 0.081 (0.023)    | 0.092 (0.020)    | 0.075 (0.022)    | <0.0001  |
|                   | D→A       | 0.095 (0.025)    | 0.114 (0.026)    | 0.084 (0.018)    | <0.0001  |
|                   | D→B       | 0.085 (0.017)    | 0.077 (0.017)    | 0.090 (0.016)    | <0.0001  |
|                   | D→C       | 0.081 (0.023)    | 0.092 (0.019)    | 0.075 (0.023)    | <0.0001  |

A, Microstate A; B, Microstate B; C, Microstate C; D, Microstate D; DRE, drug-refractory epilepsy; n, number of patients; NDRE, non-drug-refractory epilepsy group; TP, transition probabilities; →, transition probability from one microstate to another microstate.

measures the model's predictive accuracy, was 0.912 [95% confidence interval: 0.857–0.967] for the training set. For the test set, the C-index was 0.927 [95% confidence interval: 0.872–0.981].

#### CE model

In the Lasso regression, the optimal lambda value was determined when the partial likelihood deviance reached its minimum (Figure 4(b)). Ten features with nonzero Lasso coefficients underwent

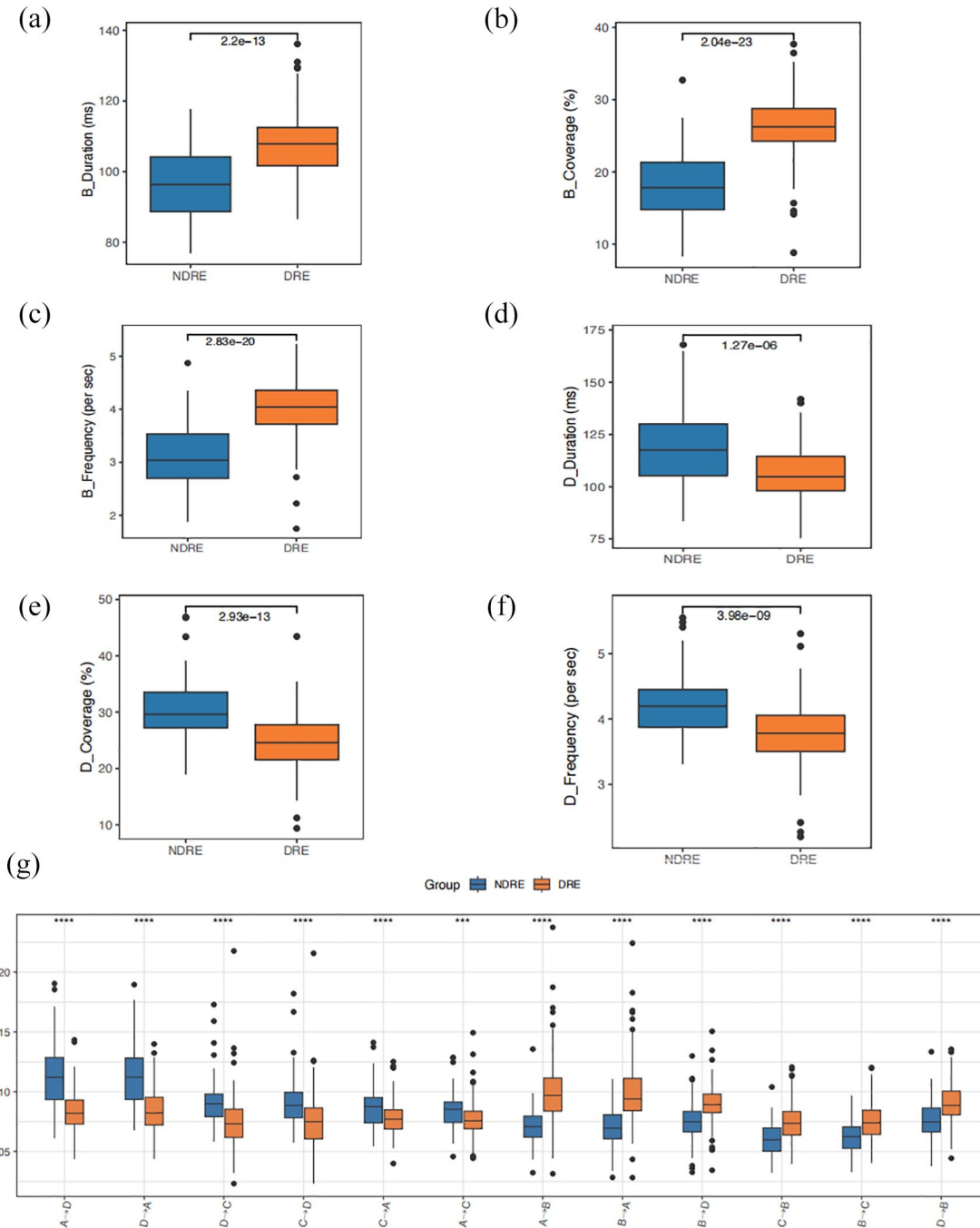


**Figure 3.** EEG microstate features. Compare the duration, frequency, coverage of each microstate, and transition probabilities between each microstate between the two groups: (a) correspond to the duration of microstate B, (b) correspond to the coverage of microstate B, (c) correspond to the frequency of microstate B, (d) correspond to the duration of microstate D, (e) correspond to the coverage of microstate D, (f) correspond to the frequency of microstate D, and (g) transition probabilities between each microstate. \* $p < 0.05$ . \*\* $p < 0.01$ . \*\*\* $p < 0.001$ . \*\*\*\* $p < 0.0001$ . DRE, drug-refractory epilepsy; EEG, electroencephalography; NDRE, non-drug-refractory epilepsy.

further analysis using Stepglm [both], resulting in the identification of a final set of eight features (Figure 4(c)). Consequently, the model included a total of eight features: duration of epilepsy,

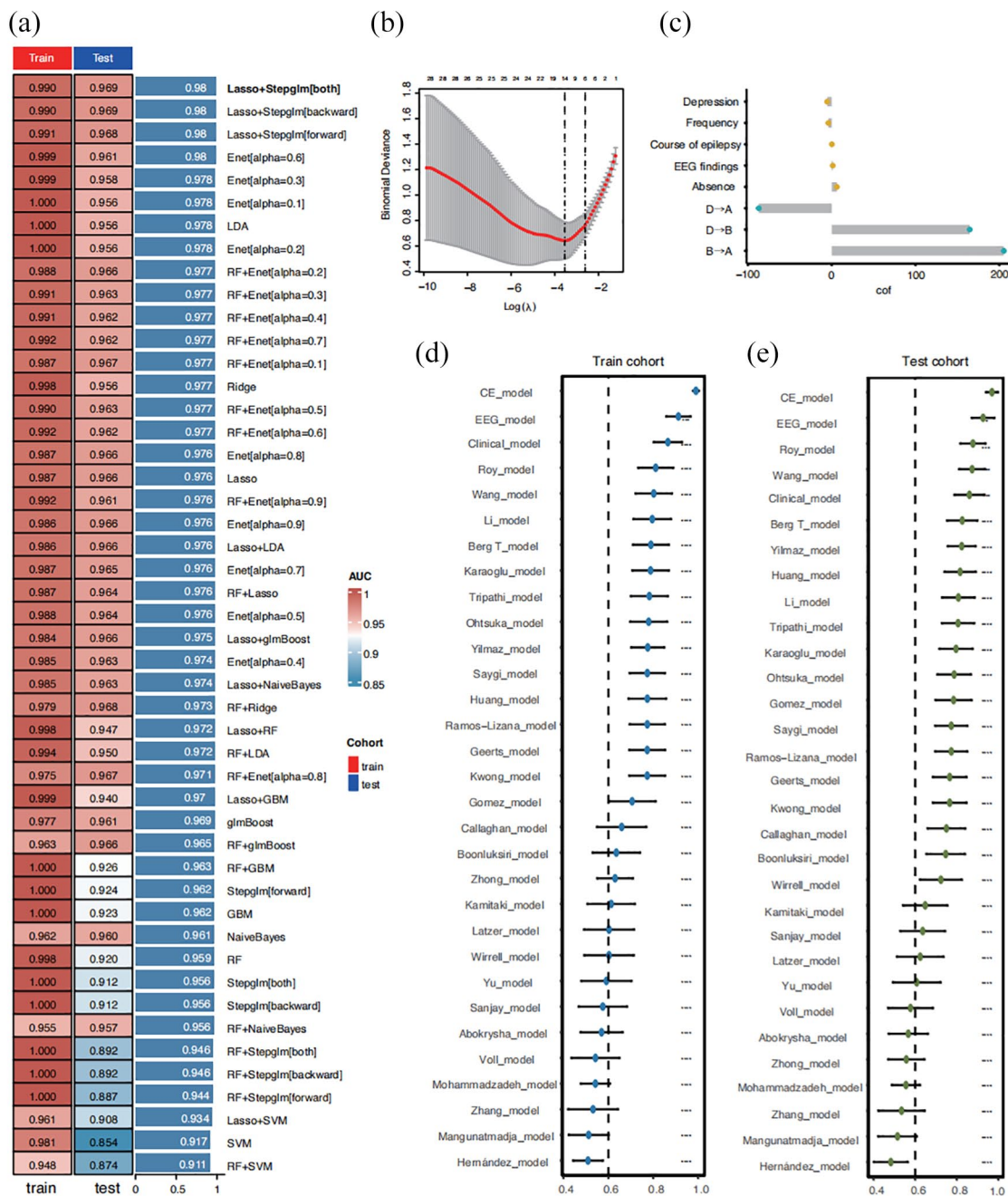


**Figure 4.** A prediction algorithm was developed and validated via the machine learning-based integrative procedure. Establish three models and compare them with other models: (a) a total of 10 machine learning algorithms and 48 algorithm combinations. The integrative algorithms included Lasso, Ridge, Enet, Stepglm, SVM, glmBoost, LDA, RF, GBM, and naïve Bayes. Further calculated the AUC of each model across all datasets, (b) the optimal lambda was obtained when the partial likelihood deviance reached the minimum value, and plot a vertical dashed line at the optimal value. The optimal lambda value yielded 10 non-zero coefficients, (c) coefficients of eight variables were finally obtained in the Stepglm [both] model, (d) C-index analysis of three models and 28 published other models in the training set, and (e) C-index analysis of three models and 28 published other models in the test set.

\* $p < 0.05$ . \*\* $p < 0.01$ . \*\*\* $p < 0.001$ . \*\*\*\* $p < 0.0001$ .

AUC, area under the curve; Enet, elastic network; GBM, generalized boosted regression model; glmBoost, generalized linear model boosting; LDA, linear discriminant analysis; RF, random forest; Stepglm, stepwise generalized linear model; SVM, support vector machine.

initial seizure frequency, EEG findings, absence epilepsy, comorbid depression, and the TPs of microstates B to A, D to A, and D to B. The model, which integrated clinical and EEG microstate information, exhibited the best performance. The C-index [95% confidence interval] for the training and test sets were 0.990 [0.978–1.000] and 0.969 [0.941–0.998], respectively.

#### *Comparison of three models and other models*

The C-indexes of the three models were compared with other models,<sup>33–60</sup> as detailed in Table 3 and Supplemental Table 1. Notably, the CE model achieved the highest C-index on both the training and test sets (Figures 4(d) and (e)).

The Brier score was used to assess the accuracy of the probability of the best-performing model, defined as the mean square deviation between the observed and predicted outcomes. The Brier scores ranged from 0 to 1.00, with 0 representing the best calibration. The Brier scores [95% confidence interval] for three models in the training set were 0.144 [0.109–0.179], 0.114 [0.075–0.152], and 0.034 [0.010–0.058]. The Brier scores [95% confidence interval] for three models in the test set were 0.144 [0.104–0.183], 0.092 [0.057–0.127], and 0.071 [0.031–0.111]. The CE model had the lowest Brier score of the three models, closest to 0, both for the training and test sets, which indicates the good performance of the constructed prediction model. Through the calibration curve, it could be observed that the predicted risk aligned well with the actual risk represented by the reference line. This indicated that the model possesses good calibration capability (Figure 5(a) and (b)).

Then, we chose CE model as the final prediction model for DRE and further constructed a corresponding nomogram. The total nomogram score was applied to obtain the sort of probability for predicting incident DRE. The duration of epilepsy, initial seizure frequency, EEG findings, absence epilepsy, comorbid depression, and the TP of microstates B–A, D–A, and D–B were included in the nomogram (Figure 5(c)). When using the nomogram, we first needed to determine the position of different variables on their respective axes and then find the corresponding points on the top axis. After adding together the point values for all variables, we drew a vertical

line downward from this total point value to predict DRE. We found that DRE was independently associated with several factors: the duration of epilepsy, initial seizure frequency, comorbid depression, and the TPs of microstates B–A, D–A, as well as D–B. The AUC values for the three models in the training set were 0.990, 0.912, and 0.865, respectively (Figure 6(a)). Similarly, the AUC values for the three models in the test set were 0.969, 0.927, and 0.861, respectively (Figure 6(b)). DCAs (Figure 6(c) and (d)) were established to confirm the clinical applicability of the nomogram. DCA showed that the prediction of DRE with the nomogram provide greater net benefits when the threshold probability was >70%.

#### **Discussion**

Despite the development and availability of over 20 different ASMs, approximately one-third of epilepsy patients struggle to achieve seizure control through medication.<sup>1,2</sup> The early identification of patients developing DRE and subsequently shifting their treatment approach toward more personalized interventions, such as ketogenic diet, surgical resection, and neuromodulation therapies,<sup>3</sup> holds significant clinical importance. To address this objective, we constructed a comprehensive predictive model based on clinical and EEG microstates features. Through C-index, AUC, calibration curve, Brier score, and DCA, this model demonstrated its superior discriminative ability, calibration, and clinical applicability. Additionally, our study innovatively visualized the application of the comprehensive prediction model through constructing a nomogram and developing a web calculator ([https://fydxh.shinyapps.io/CE\\_model\\_of\\_DRE/](https://fydxh.shinyapps.io/CE_model_of_DRE/)), providing a novel approach for rapidly obtaining real-time predictions of the probability of DRE occurrence. In our study, a total of 45 clinical feature variables and EEG microstate feature variables were included. Correlation analysis of variables revealed correlations among some of them. To address collinearity issues and overfitting of the data, a combination of Lasso and Stepglm [both] algorithms was employed for variable selection, effectively resolving collinearity and interaction problems. Additionally, 10-fold cross validation was utilized to ensure the model's generalization ability and accuracy. These methods contributed to constructing a simplified model, enhancing

**Table 3.** Comparison of three DRE prediction models from this study with models reported in previous research.

| Models                         | Training set |             | Test set  |             |
|--------------------------------|--------------|-------------|-----------|-------------|
|                                | C-index      | 95% CI      | C-index   | 95% CI      |
| CE model                       | 0.99         | 0.978–1.00  | 0.969     | 0.941–0.998 |
| EEG model                      | 0.912***     | 0.858–0.966 | 0.927*    | 0.872–0.981 |
| Clinical model                 | 0.865****    | 0.802–0.928 | 0.861***  | 0.788–0.934 |
| Seker Yilmaz <sup>60</sup>     | 0.775****    | 0.702–0.849 | 0.824**** | 0.757–0.891 |
| Kwong <sup>33</sup>            | 0.772****    | 0.693–0.853 | 0.766**** | 0.685–0.847 |
| Ohtsuka <sup>58</sup>          | 0.779****    | 0.697–0.862 | 0.788**** | 0.707–0.868 |
| Wirrell <sup>59</sup>          | 0.603****    | 0.492–0.713 | 0.724**** | 0.623–0.824 |
| Berg <sup>57</sup>             | 0.789****    | 0.709–0.869 | 0.826**** | 0.754–0.899 |
| Sanjay <sup>56</sup>           | 0.575****    | 0.467–0.683 | 0.636**** | 0.529–0.744 |
| Ramos-Lizana <sup>34</sup>     | 0.773****    | 0.695–0.852 | 0.774**** | 0.696–0.851 |
| Geerts <sup>35</sup>           | 0.773****    | 0.693–0.853 | 0.766**** | 0.685–0.847 |
| Tripathi <sup>36</sup>         | 0.782****    | 0.700–0.865 | 0.806**** | 0.729–0.884 |
| Huang <sup>37</sup>            | 0.773****    | 0.689–0.857 | 0.816**** | 0.741–0.892 |
| Saygi <sup>38</sup>            | 0.773****    | 0.695–0.852 | 0.774**** | 0.696–0.851 |
| Gomez-Ibañez <sup>39</sup>     | 0.706****    | 0.601–0.810 | 0.785**** | 0.698–0.872 |
| Mangunatmadja <sup>40</sup>    | 0.512****    | 0.423–0.601 | 0.515**** | 0.422–0.608 |
| Roy <sup>41</sup>              | 0.811****    | 0.732–0.889 | 0.878***  | 0.817–0.938 |
| Li <sup>42</sup>               | 0.795****    | 0.711–0.879 | 0.808**** | 0.730–0.886 |
| Karaoğlu <sup>43</sup>         | 0.787****    | 0.706–0.869 | 0.797**** | 0.717–0.876 |
| Mohammadzadeh <sup>44</sup>    | 0.542****    | 0.477–0.607 | 0.555**** | 0.488–0.623 |
| Voll <sup>45</sup>             | 0.542****    | 0.435–0.649 | 0.578**** | 0.470–0.685 |
| Zhang <sup>46</sup>            | 0.532****    | 0.421–0.642 | 0.534**** | 0.423–0.645 |
| Boonluksiri <sup>47</sup>      | 0.635****    | 0.530–0.741 | 0.747**** | 0.654–0.840 |
| Orozco-Hernández <sup>48</sup> | 0.509****    | 0.443–0.575 | 0.483**** | 0.401–0.565 |
| Zhong <sup>49</sup>            | 0.630****    | 0.550–0.709 | 0.557**** | 0.471–0.644 |
| Tokatly Latzer <sup>50</sup>   | 0.603****    | 0.492–0.714 | 0.624**** | 0.512–0.737 |
| Callaghan <sup>51</sup>        | 0.659****    | 0.549–0.769 | 0.750**** | 0.660–0.841 |
| Wang <sup>55</sup>             | 0.802****    | 0.721–0.883 | 0.874***  | 0.812–0.936 |
| Abokrysha <sup>52</sup>        | 0.570****    | 0.476–0.663 | 0.567**** | 0.472–0.661 |
| Yu <sup>53</sup>               | 0.591****    | 0.479–0.703 | 0.607**** | 0.493–0.722 |
| Kamitaki <sup>54</sup>         | 0.612****    | 0.507–0.718 | 0.648**** | 0.541–0.755 |

\* $p < 0.05$ . \*\* $p < 0.01$ . \*\*\* $p < 0.001$ . \*\*\*\* $p < 0.0001$ .

CE model, clinical + EEG comprehensive predictive model; C-index, concordance index; 95% CI, 95% confidence interval; DRE, drug-refractory epilepsy; EEG model, EEG microstate model; EEG, electroencephalography.

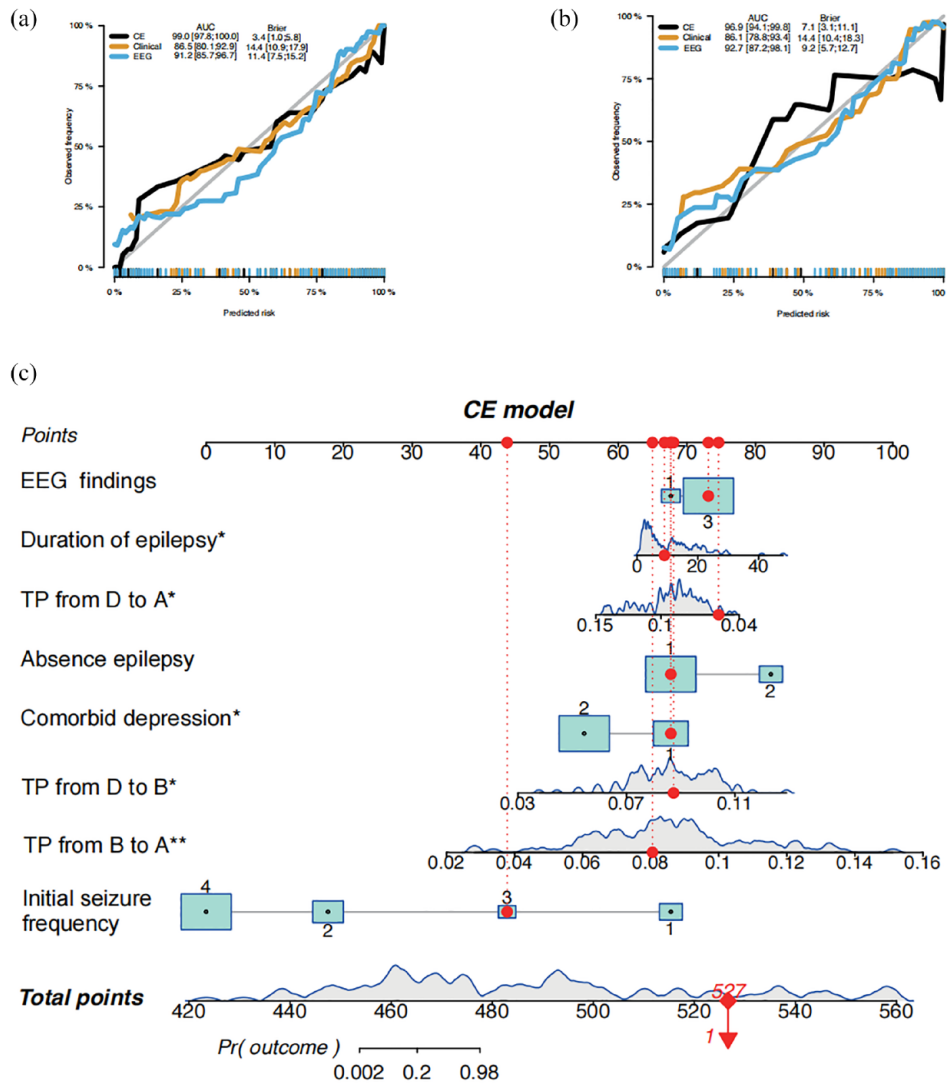


**Figure 5.** Establishment of nomograms for predicting patients with DRE: (a) calibration curve of the three models in the training set, (b) calibration curve of the three models in the test set, and (c) Nomogram for predicting patients with DRE using the duration of epilepsy, initial seizure frequency, EEG findings, absence epilepsy, comorbid depression, and the transition probability of microstates B–A, D–A, and D–B.

\* $p < 0.05$ . \*\* $p < 0.01$ .

DRE, drug-refractory epilepsy; EEG, electroencephalography.

model interpretability, and optimizing overall performance.<sup>31,32</sup>

Kuzmanovski *et al.*<sup>61</sup> indicated that a longer duration of epilepsy is associated with an increased likelihood of drug resistance. Consistent with this observation, our study reports that patients diagnosed with DRE experienced epilepsy for an average of 6 years longer than those in the NDRE group. This further confirms that an extended duration of epilepsy

may increase the incidence of DRE. This increase could be associated with the heightened complexity of treatment and the broader variety of ASMs used as the duration of epilepsy extends. A meta-analysis conducted in 2019 revealed that EEG abnormalities, including slow waves and epileptiform discharges, are predictive factors for DRE.<sup>62</sup> Additionally, focal slowing in EEG has been demonstrated as a clinical risk factor that predicts DRE in children with cerebral palsy.<sup>50</sup> In this study, compared to the NDRE

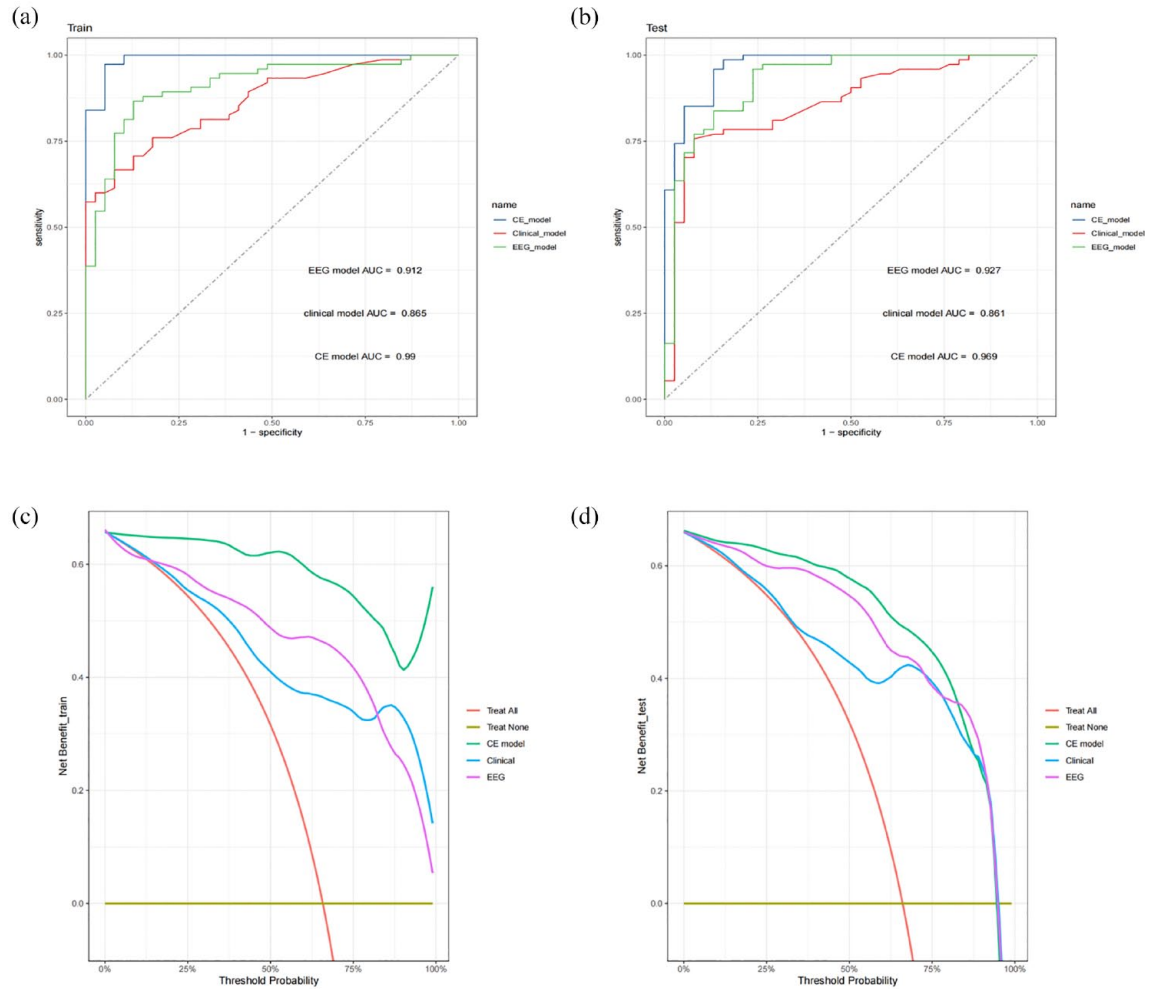


**Figure 6.** The ROC curves and DCA demonstrated the accuracy and clinical applicability of these prediction models: (a) ROC curve for the three models in the training set, (b) ROC curve for the three models in the test set, (c) decision curve for the three models in the training set, and (d) decision curve for the three models in the test set.  
DCA, decision curve analysis.

group, the DRE group exhibited a higher proportion of EEG with abnormal background and epileptiform discharges, consistent with the results of previous studies. This suggests that EEG abnormalities may serve as an indicator of the occurrence of DRE. The initial seizure frequency is considered a strong and independent factor in predicting the development of DRE.<sup>37,45</sup> Furthermore, a high seizure frequency indicates a more severe disease condition and suggests a more severe form of epilepsy.<sup>43</sup> In our study, the DRE group had a higher initial seizure frequency, consistent with the results of previous studies. This could be due to the loss of neurons in the hippocampus and the sprouting of mossy fibers caused by repeated seizures, potentially

leading to the formation of recurrent excitatory circuits, thereby promoting the occurrence of DRE.<sup>43</sup>

Psychological disorders are common comorbidities in patients with epilepsy, involving a range of complex neurobiological mechanisms.<sup>63</sup> Among these, depression is the most prevalent,<sup>64</sup> and the coexistence of depression is significantly associated with an increased risk of developing DRE.<sup>65</sup> In studies of patients with refractory epilepsy, about 30% of those with DRE also suffer from depression, with a prevalence rate of approximately 35% in this specific population.<sup>22,64</sup> This rate is significantly higher than the prevalence of depression in the general population,



underscoring the importance of identifying and treating depressive disorders in patients with DRE.<sup>22</sup> In our study, the occurrence of comorbid depression was higher among patients with DRE compared to those without DRE, consistent with past research, and further highlighted the significance of coexisting depression in the development of DRE. Kamitaki *et al.*<sup>54</sup> suggested that absence seizures serve as an independent risk factor for DRE. In our study, we found a higher proportion of absence seizures in the DRE group. The presence of absence seizures may increase the risk of developing DRE. However, further research is needed to explore the exact association between absence seizures and drug-resistant epilepsy.

Recent studies have highlighted the significant potential of EEG microstates in epilepsy and its treatment.<sup>66,67</sup> Jiang *et al.*<sup>66</sup> found that patients with idiopathic generalized epilepsy (IGE) who experienced seizures in the past 6 months showed higher frequencies and coverage of microstate A and lower of microstate C, with no significant differences in microstates B and D. Sun *et al.*<sup>67</sup> observed significant changes in the temporal characteristics of the four typical EEG microstates in patients with temporal lobe epilepsy and depression. Microstate A is associated with brain activity in the temporal cortex and left insula.<sup>14</sup> Microstate B is related to the visual network,<sup>14</sup> and an increase in the average duration of microstate B has been found to be associated with cognitive fatigue.<sup>14</sup> Alzheimer's disease (AD) and bipolar affective disorder are the most typical examples, with patients of both diseases showing increased connectivity in the auditory and visual networks, and cognitive impairment leading to a more visual-oriented brain activity.<sup>68</sup> In our study, DRE group showed increased average duration, frequency, and coverage of microstate B, while these parameters of microstate D decreased. Moreover, the TP from microstate D to B increased, consistent with previous studies. This result may reflect cognitive impairment in DRE patients due to uncontrolled long-term seizure activity, prompting a shift in brain activity toward visual functional areas. It is speculated that the frequent occurrence of microstate B in DRE patients may come at the expense of microstate D.<sup>14</sup>

Research indicates that microstate C is associated with the salience network, and a decrease in the frequency of microstate C may result from declining cognitive levels, cognitive fatigue, and epileptic seizures.<sup>69</sup> In our study, the duration of microstate

C decreased in the DRE group, consistent with previous research, which may suggest obstacles in the patients' cognitive-emotional assessment of the environment.<sup>69</sup> Abnormalities in microstate D are associated with decreased attention, and the severity of the condition is negatively correlated with the average duration and frequency of microstate D.<sup>70</sup> Baldini *et al.*<sup>71</sup> reported a decrease in duration, coverage, and frequency of microstate D in patients with temporal lobe epilepsy, a trend also observed in our study, indicating potential attention deficits in patients with DRE. The TPs between EEG microstates are non-random and hold potential importance for understanding brain dynamics. Our study showed increased TPs (B–A, D–B) in the DRE group compared to the NDRE group, with lower transitions from D to A in the DRE group. These differences may reflect fundamental distinctions in brain activity patterns between patients with DRE and NDRE, implying different neural network dynamics and brain connectivity patterns. When combined with our previous assertion that cognitive dysfunction (reduced microstate D, increased D to B transitions) could enhance the functionality of microstate B, we can hypothesize that increased TPs from B to A may result from disease-induced dysfunctional connectivity between neural networks. This contrast with alterations in TPs from D to A and D to B could potentially enhance connectivity between microstates A and B, thereby increasing TPs.<sup>70</sup> These findings imply that the TPs between different microstates can all serve as important reference indicators for evaluating DRE. Future research should focus on exploring the relationship between these changes in microstate TPs and susceptibility to epileptic seizures, drug responsiveness, and brain network function.

### Limitations

Our study has several limitations. First, the retrospective nature of the study introduces selection bias. To address this issue, future prospective studies are necessary. Second, our study lacks a formal power analysis for sample size calculation. Future studies should include a formal power analysis to determine the optimal sample size. Additionally, the sample size is small and limited to Asian individuals, which may affect the generalizability of our findings. Larger and multicenter studies involving diverse populations are needed. In addition, we selected other models from the PubMed database to compare with the three

DRE prediction models, which may introduce selection bias. Finally, future research should focus on implementing these markers in clinical practice to establish accurate models for predicting DRE.

### Conclusion

Our research shows that predicting DRE is possible using a comprehensive model that combines clinical and EEG microstate features. More evaluation is needed to determine its applicability in clinical settings.

### Declarations

#### *Ethics approval and consent to participate*

The Ethics Committee of Fujian Medical University Union Hospital granted approval for the prospective clinical research project (approval code 2017KY085). In addition, a separate approval was obtained for the now-presented retrospective analysis of EEG data from patients with drug-refractory epilepsy (approval code: 2022YF018-01). Written informed consent was obtained from all participants in accordance with the principles set forth in the Helsinki Declaration.

#### *Consent for publication*

Not applicable.

#### *Author contributions*

**Jinying Zhang:** Conceptualization; Investigation; Methodology; Software; Validation; Visualization; Writing – original draft.

**Chaofeng Zhu:** Funding acquisition; Project administration; Supervision; Writing – review & editing.

**Juan Li:** Data curation.

**Luyan Wu:** Data curation.

**Yuying Zhang:** Methodology; Supervision.

**Huapin Huang:** Conceptualization; Funding acquisition; Project administration; Resources; Supervision; Writing – review & editing.

**Wanhui Lin:** Supervision.

#### *Acknowledgements*

We are grateful to all the participants for their valuable information, cooperation, and participation.

#### *Funding*

The authors disclosed receipt of the following financial support for the research, authorship, and/or publication of this article: This study was supported by Excellent Young Scholars Cultivation Project of Fujian Medical University Union Hospital (2022XH037), the Youth Project of National Natural Science Foundation of China (Grant No. 82201604), Natural Science Foundation of Fujian Province, China (Grant No. 2023J05148), and National Key Clinical Specialty (21281003).

#### *Competing interests*

The authors declare that there is no conflict of interest.

#### *Availability of data and materials*

The datasets used or analyzed during the current study are available from the corresponding author on reasonable request.

#### ORCID iD

Wanhui Lin  <https://orcid.org/0000-0002-8537-8840>

#### Supplemental material

Supplemental material for this article is available online.

#### References

1. Janmohamed M, Brodie MJ and Kwan P. Pharmacoresistance - Epidemiology, mechanisms, and impact on epilepsy treatment. *Neuropharmacology* 2020; 168: 107790.
2. Kwan P, Arzimanoglou A, Berg AT, et al. Definition of drug resistant epilepsy: consensus proposal by the ad hoc Task Force of the ILAE Commission on Therapeutic Strategies [published correction appears in *Epilepsia* 2010; 51(9): 1922]. *Epilepsia* 2010; 51(6): 1069–1077.
3. Anyanwu C and Motamedi GK. Diagnosis and surgical treatment of drug-resistant epilepsy. *Brain Sci* 2018; 8(4): 49.
4. Wirrell EC. Predicting pharmacoresistance in pediatric epilepsy. *Epilepsia* 2013; 54(Suppl. 2): 19–22.
5. Asadi-Pooya AA, Brigo F, Lattanzi S, et al. Adult epilepsy. *Lancet* 2023; 402(10399): 412–424.
6. Antonakakis M, Dimitriadis SI, Zervakis M, et al. Aberrant whole-brain transitions and dynamics

- of spontaneous network microstates in mild traumatic brain injury. *Front Comput Neurosci* 2020; 13: 90.
7. Tait L and Zhang J. +microstate: a MATLAB toolbox for brain microstate analysis in sensor and cortical EEG/MEG. *Neuroimage* 2022; 258: 119346.
  8. Koenig T, Marti-Lopez F and Valdes-Sosa P. Topographic time-frequency decomposition of the EEG. *Neuroimage* 2001; 14(2): 383–390.
  9. Cao J, Zhao Y, Shan X, et al. Brain functional and effective connectivity based on electroencephalography recordings: a review. *Hum Brain Mapp.* 2022; 43(2): 860–879.
  10. Khanna A, Pascual-Leone A, Michel CM, et al. Microstates in resting-state EEG: current status and future directions. *Neurosci Biobehav Rev* 2015; 49: 105–113.
  11. Gao F, Jia H, Wu X, et al. Altered resting-state EEG microstate parameters and enhanced spatial complexity in male adolescent patients with mild spastic diplegia. *Brain Topogr* 2017; 30(2): 233–244.
  12. Michel CM and Koenig T. EEG microstates as a tool for studying the temporal dynamics of whole-brain neuronal networks: a review. *Neuroimage* 2018; 180(Pt B): 577–593.
  13. Koenig T, Prichet L, Lehmann D, et al. Millisecond by millisecond, year by year: normative EEG microstates and developmental stages. *Neuroimage* 2002; 16(1): 41–48.
  14. Wang H, Yin N and Xu G. Progress in the Analysis and application of microstates in electroencephalography. *J Biomed Eng* 2023; 40(01): 163–170.
  15. Britz J, Van De Ville D and Michel CM. BOLD correlates of EEG topography reveal rapid resting-state network dynamics. *Neuroimage* 2010; 52(4): 1162–1170.
  16. Yuan H, Zotev V, Phillips R, et al. Spatiotemporal dynamics of the brain at rest—exploring EEG microstates as electrophysiological signatures of BOLD resting state networks. *Neuroimage* 2012; 60(4): 2062–2072.
  17. Vaughan HG Jr. The neural origins of human event-related potentials. *Ann N Y Acad Sci* 1982; 388: 125–138.
  18. Irisawa S, Isotani T, Yagy T, et al. Increased omega complexity and decreased microstate duration in nonmedicated schizophrenic patients. *Neuropsychobiology* 2006; 54(2): 134–139.
  19. Nishida K, Morishima Y, Yoshimura M, et al. EEG microstates associated with salience and frontoparietal networks in frontotemporal dementia, schizophrenia and Alzheimer’s disease. *Clin Neurophysiol* 2013; 124(6): 1106–1114.
  20. Drissi NM, Szakács A, Witt ST, et al. Altered brain microstate dynamics in adolescents with narcolepsy [published correction appears in *Front Hum Neurosci* 2019 Nov 06; 13: 385]. *Front Hum Neurosci* 2016; 10: 369.
  21. Liu H, Tang H, Wei W, et al. Altered peri-seizure EEG microstate dynamics in patients with absence epilepsy. *Seizure* 2021; 88: 15–21.
  22. Li Z, Cao W, Sun H, et al. Potential clinical and biochemical markers for the prediction of drug-resistant epilepsy: a literature review. *Neurobiol Dis* 2022; 174: 105872.
  23. Jia X, Wang Z, Huang F, et al. A comparison of the Mini-Mental State Examination (MMSE) with the Montreal Cognitive Assessment (MoCA) for mild cognitive impairment screening in Chinese middle-aged and older population: a cross-sectional study. *BMC Psychiatry* 2021; 21(1): 485.
  24. Tang X, Lu Z, Hu D, et al. Influencing factors for prenatal stress, anxiety and depression in early pregnancy among women in Chongqing, China. *J Affect Disord* 2019; 253: 292–302.
  25. Nagabhushan Kalburgi S, Kleinert T, Aryan D, et al. MICROSTATELAB: the EEGLAB toolbox for resting-state microstate analysis. *Brain Topogr.* Epub ahead of print September 11, 2023. DOI: 10.1007/s10548-023-01003-5.
  26. Delorme A and Makeig S. EEGLAB: an open source toolbox for analysis of single-trial EEG dynamics including independent component analysis. *J Neurosci Methods* 2004; 134(1): 9–21.
  27. Zhu C, Li J, Wei D, et al. Intrinsic brain activity differences in perampal-responsive and non-responsive drug-resistant epilepsy patients: an EEG microstate analysis. *Ther Adv Neurol Disord* 2024; 17: 17562864241227293.
  28. Cai Y, Chen S, Chen Y, et al. Altered resting-state EEG microstate in idiopathic sudden sensorineural hearing loss patients with tinnitus. *Front Neurosci* 2019; 13: 443.
  29. Kikuchi M, Koenig T, Munesue T, et al. EEG microstate analysis in drug-naive patients with panic disorder. *PLoS One* 2011; 6(7): e22912.
  30. Pascual-Marqui RD, Michel CM and Lehmann D. Segmentation of brain electrical activity into microstates: model estimation and validation. *IEEE Trans Biomed Eng* 1995; 42(7): 658–665.

31. Wang Y, Bu Z, Li Y, et al. Methods and comparison of variable selection in clinical prediction models [J]. *Modern Trad Chin Med Clin* 2024; 31(02): 6–12.
32. Liang Z, Li Z, Lai K, et al. Evaluation of predictive model generalization capability and its implementation in R software using 10-fold cross-validation. *Chin Hospital Stat* 2020; 27(4): 289–292.
33. Kwong KL, Sung WY, Wong SN, et al. Early predictors of medical intractability in childhood epilepsy. *Pediatr Neurol* 2003; 29(1): 46–52.
34. Ramos-Lizana J, Aguilera-López P, Aguirre-Rodríguez J, et al. Early prediction of refractory epilepsy in childhood. *Seizure* 2009; 18(6): 412–416.
35. Geerts A, Arts WF, Stroink H, et al. Course and outcome of childhood epilepsy: a 15-year follow-up of the Dutch Study of Epilepsy in Childhood. *Epilepsia* 2010; 51(7): 1189–1197.
36. Tripathi M, Padhy UP, Vibha D, et al. Predictors of refractory epilepsy in north India: a case-control study. *Seizure* 2011; 20(10): 779–783.
37. Huang L, Li S, He D, et al. A predictive risk model for medical intractability in epilepsy. *Epilepsy Behav* 2014; 37: 282–286.
38. Saygi S, Erol İ and Alehan F. Early clinical predictors of intractable epilepsy in childhood. *Turk J Med Sci* 2014; 44(3): 490–495.
39. Gomez-Ibañez A, McLachlan RS, Mirsattari SM, et al. Prognostic factors in patients with refractory idiopathic generalized epilepsy. *Epilepsy Res* 2017; 130: 69–73.
40. Mangunatmadja I, Indra RM, Widodo DP, et al. Risk factors for drug resistance in epileptic children with age of onset above five years: a case-control study. *Behav Neurol* 2021; 2021: 9092824.
41. Roy PL, Ronquillo LH, Ladino LD, et al. Risk factors associated with drug resistant focal epilepsy in adults: a case control study. *Seizure* 2019; 73: 46–50.
42. Li N, Li J, Chen Y, et al. Treatment outcome and risk factors of adult newly diagnosed epilepsy: a prospective hospital-based study in Northeast China. *Front Neurol* 2021; 12: 747958.
43. Karaoğlu P, Yaş U, Polat Aİ, et al. Clinical predictors of drug-resistant epilepsy in children. *Turk J Med Sci* 2021; 51(3): 1249–1252.
44. Mohammadzadeh P and Nazarboghi S. The prevalence of drug-resistant-epilepsy and its associated factors in patients with epilepsy. *Clin Neurol Neurosurg* 2022; 213: 107086.
45. Voll A, Hernández-Ronquillo L, Buckley S, et al. Predicting drug resistance in adult patients with generalized epilepsy: a case-control study. *Epilepsy Behav* 2015; 53: 126–130.
46. Zhang Y, Yu N, Su L, et al. A prospective cohort study of prognosis for newly diagnosed epilepsy in east China. *BMC Neurol* 2013; 13: 116.
47. Boonluksiri P, Visuthibhan A and Katanyuwong K. Clinical prediction rule of drug resistant epilepsy in children. *J Epilepsy Res* 2015; 5(2): 84–88.
48. Orozco-Hernández JP, Quintero-Moreno JF, Marín-Medina DS, et al. Multivariable prediction model of drug resistance in adult patients with generalized epilepsy from Colombia: a case-control study. *Epilepsy Behav* 2018; 88: 176–180.
49. Zhong R, Chen Q, Li N, et al. Psychiatric symptoms predict drug-resistant epilepsy in newly treated patients. *Seizure* 2022; 103: 86–91.
50. Tokatly Latzer I, Blumovich A, Sagi L, et al. Prediction of drug-resistant epilepsy in children with cerebral palsy. *J Child Neurol* 2020; 35(3): 187–194.
51. Callaghan B, Schlesinger M, Rodemer W, et al. Remission and relapse in a drug-resistant epilepsy population followed prospectively. *Epilepsia* 2011; 52(3): 619–626.
52. Abokrysha NT, Taha N, Shamloul R, et al. Clinical, radiological and electrophysiological predictors for drug-resistant epilepsy. *Egypt J Neurol Psychiatr Neurosurg* 2023; 59(1): 44.
53. Yu T, Liu X, Sun L, et al. Risk factors for Drug-resistant Epilepsy (DRE) and a nomogram model to predict DRE development in post-traumatic epilepsy patients. *CNS Neurosci Ther* 2022; 28(10): 1557–1567.
54. Kamitaki BK, Janmohamed M, Kandula P, et al. Clinical and EEG factors associated with antiseizure medication resistance in idiopathic generalized epilepsy. *Epilepsia* 2022; 63(1): 150–161.
55. Wang B, Han X, Yang S, et al. An integrative prediction algorithm of drug-refractory epilepsy based on combined clinical-EEG functional connectivity features. *J Neurol* 2022; 269(3): 1501–1514.
56. Chawla S, Aneja A, Kashyap R, et al. Etiology and clinical predictors of intractable epilepsy. *Pediatric Neurol* 2002; 27(3): 186–191.

57. Berg AT, Shinnar S, Levy SR, et al. Early development of intractable epilepsy in children: a prospective study [published correction appears in *Neurology* 2001 Sep 11; 57(5): 939]. *Neurology* 2001; 56(11): 1445–1452.
58. Ohtsuka Y, Yoshinaga H, Kobayashi K, et al. Predictors and underlying causes of medically intractable localization-related epilepsy in childhood *Pediatr Neurol* 2001; 24(3): 209–213.
59. Wirrell E, Wong-Kisiel L, Mandrekar J, et al. Predictors and course of medically intractable epilepsy in young children presenting before 36 months of age: a retrospective, population-based study. *Epilepsia* 2012; 53(9): 1563–1569.
60. Seker Yilmaz B, Okuyaz C and Komur M. Predictors of intractable childhood epilepsy. *Pediatr Neurol* 2013; 48(1): 52–55.
61. Kuzmanovski I, Cvetkovska E, Babunovska M, et al. Seizure outcome following medical treatment of mesial temporal lobe epilepsy: clinical phenotypes and prognostic factors. *Clin Neurol Neurosurg* 2016; 144: 91–95.
62. Xue-Ping W, Hai-Jiao W, Li-Na Z, et al. Risk factors for drug-resistant epilepsy: a systematic review and meta-analysis. *Medicine (Baltimore)* 2019; 98(30): e16402.
63. Hitiris N, Mohanraj R, Norrie J, et al. Predictors of pharmaco-resistant epilepsy. *Epilepsy Res* 2007; 75(2–3): 192–196.
64. D'Alessio L, Mesarosova L, Anink JJ, et al. Reduced expression of the glucocorticoid receptor in the hippocampus of patients with drug-resistant temporal lobe epilepsy and comorbid depression. *Epilepsia* 2020; 61(8): 1595–1605.
65. Scévola L, Sarudiansky M, Lanzillotti A, et al. To what extent does depression influence quality of life of people with pharmaco-resistant epilepsy in Argentina?. *Epilepsy Behav* 2017; 69: 133–138.
66. Jiang Y, Zhu M, Hu Y, et al. Altered resting-state electroencephalography microstates in idiopathic generalized epilepsy: a prospective case–control study. *Front Neurol* 2021; 12: 710952.
67. Sun Y, Ren G, Ren J, et al. Intrinsic brain activity in temporal lobe epilepsy with and without depression: insights from EEG microstates. *Front Neurol* 2021; 12: 753113.
68. Vellante F, Ferri F, Baroni G, et al. Euthymic bipolar disorder patients and EEG microstates: a neural signature of their abnormal self-experience?. *J Affect Disord* 2020; 272: 326–334.
69. Chu CG, Wang X, Cai LH, et al. Spatiotemporal EEG microstate analysis in drug-free patients with Parkinson's disease. *NeuroImage Clin* 2020; 25: 102132.
70. Fang S, Zhu C, Zhang J, et al. EEG microstates in epilepsy with and without cognitive dysfunction: alteration in intrinsic brain activity. *Epilepsy Behav* 2024; 154: 109729.
71. Baldini S, Duma GM, Danieli A, et al. Electroencephalographic microstates as a potential neurophysiological marker differentiating bilateral from unilateral temporal lobe epilepsy. *Epilepsia* 2024; 65: 664–674.